Struck, M., Andermann, C., Hovius, N., Korup, O., Turowski, J., Bista, R., Pandit, H. P., Dahal, R. K. (2015): Monsoonal hillslope processes determine grain-size-specific suspended sediment fluxes in a trans-Himalayan river. - *Geophysical Research Letters*, *42*, 7, p. 2302-2308.

DOI: http://doi.org/10.1002/2015GL063360

AGU PUBLICATIONS

Geophysical Research Letters

RESEARCH LETTER
10.1002/2015GL063360

Key Points:
- Suspended sediment coarsens downstream through the Himalayas during monsoon
- Hillslope supply determines characteristic river sediments granulometry
- Fine grained sediments are predominantly sourced from the arid Tibetan Plateau

Supporting Information:
- Text S4, Figures S1, S2, S5, S6, S8, and S9, and Tables S3 and S7

Correspondence to:
C. Andermann,
christoff.andermann@gfz-potsdam.de

Citation:
Struck, M., C. Andermann, N. Hovius, O. Korup, J. M. Turowski, R. Bista, H. P. Pandit, and R. K. Dahal (2015), Monsoonal hillslope processes determine grain size-specific suspended sediment fluxes in a trans-Himalayan river, *Geophys. Res. Lett.*, *42*, 2302–2308, doi:10.1002/2015GL063360.

Received 4 FEB 2015
Accepted 18 MAR 2015
Accepted article online 24 MAR 2015
Published online 14 APR 2015

Monsoonal hillslope processes determine grain size-specific suspended sediment fluxes in a trans-Himalayan river

Martin Struck[1,2], Christoff Andermann[1], Niels Hovius[1], Oliver Korup[3], Jens M. Turowski[1,4], Raj Bista[5], Hari P. Pandit[6], and Ranjan K. Dahal[7]

[1]GFZ German Research Centre for Geosciences, Potsdam, Germany, [2]School of Earth and Environmental Sciences, University of Wollongong, Wollongong, New South Wales, Australia, [3]Institute of Earth and Environmental Sciences, University of Potsdam, Potsdam, Germany, [4]Swiss Federal Research Institute WSL, Zurich, Switzerland, [5]Nepal Electricity Authority, Kathmandu, Nepal, [6]Institute of Engineering, Tribhuvan University, Kathmandu, Nepal, [7]Department of Geology, Tri-Chandra Multiple Campus, Tribhuvan University, Kathmandu, Nepal

Abstract Sediments in rivers record the dynamics of erosion processes. While bulk sediment fluxes are easily and routinely obtained, sediment caliber remains underexplored when inferring erosion mechanisms. Yet sediment grain size distributions may be the key to discriminating their origin. We have studied grain size-specific suspended sediment fluxes in the Kali Gandaki, a major trans-Himalayan river. Two strategically located gauging stations enable tracing of sediment caliber on either side of the Himalayan orographic barrier. The data show that fine sediment input into the northern headwaters is persistent, while coarse sediment comes from the High Himalayas during the summer monsoon. A temporally matching landslide inventory similarly indicates the prominence of monsoon-driven hillslope mass wasting. Thus, mechanisms of sediment supply can leave strong traces in the fluvial caliber, which could project well beyond the mountain front and add to the variability of the sedimentary record of orogen erosion.

1. Introduction

The grain size of river sediments is set by supply from interfluves, in-channel comminution, and sorting. While progressive downstream fining of alluvial river sediments is attributed to in-channel processes of selective transport [e.g., *Paola and Seal*, 1995], the granulometry of erosional rivers appears to be less regular due to external influences such as variations in hillslope sediment supply [*Brummer and Montgomery*, 2003; *Attal and Lavé*, 2006; *Marshall and Sklar*, 2012]. Most material building sedimentary archives in distant depositional basins is carried in suspension [*Turowski et al*., 2010]. In mountain rivers, suspended sediment transport is rarely limited by the transport capacity [e.g., *Andermann et al*., 2012a], and thus, the effects of episodic sediment supply may be expressed in the quantity of suspended material, as well as its caliber, which can be easily measured. Although the source geology and mechanisms of sediment mobilization and transfer likely feature a granulometric fingerprint, the caliber is underexplored for geomorphological purposes. Yet this may be useful in mountain belts such as the Himalayas where the links between distributed erosion and fluvial sediment transfer remain underconstrained. On the southern side of the mountain belt hillslope sediment delivery to river channels promotes high monsoonal sediment fluxes [e.g., *Gabet et al*., 2008; *Andermann et al*., 2012a; *Wulf et al*., 2012]. Less is known about the processes that supply sediment to Himalayan rivers on the northern, lee side of the orographic barrier, and it is generally assumed that these trans-Himalayan compartments contribute little to the clastic fluxes at the mountain front [e.g., *Wulf et al*., 2012].

The aim of this study is to show that suspended sediment caliber contains information about supply mechanisms of sediments to rivers and about their mobilization on hillslopes. Therefore, we analyze daily discharge and suspended sediment concentrations and grain size data from two hydrometric stations on the Kali Gandaki (KG), one of the major trans-Himalayan rivers (Figure 1). One station sits at the edge of the Tibetan Plateau, within the topographic transition from the dry, high-elevation zone to the monsoon-drenched southern Himalayan front (Figures 1 and 1 b). The second station integrates both the arid and humid portions of the KG watershed.

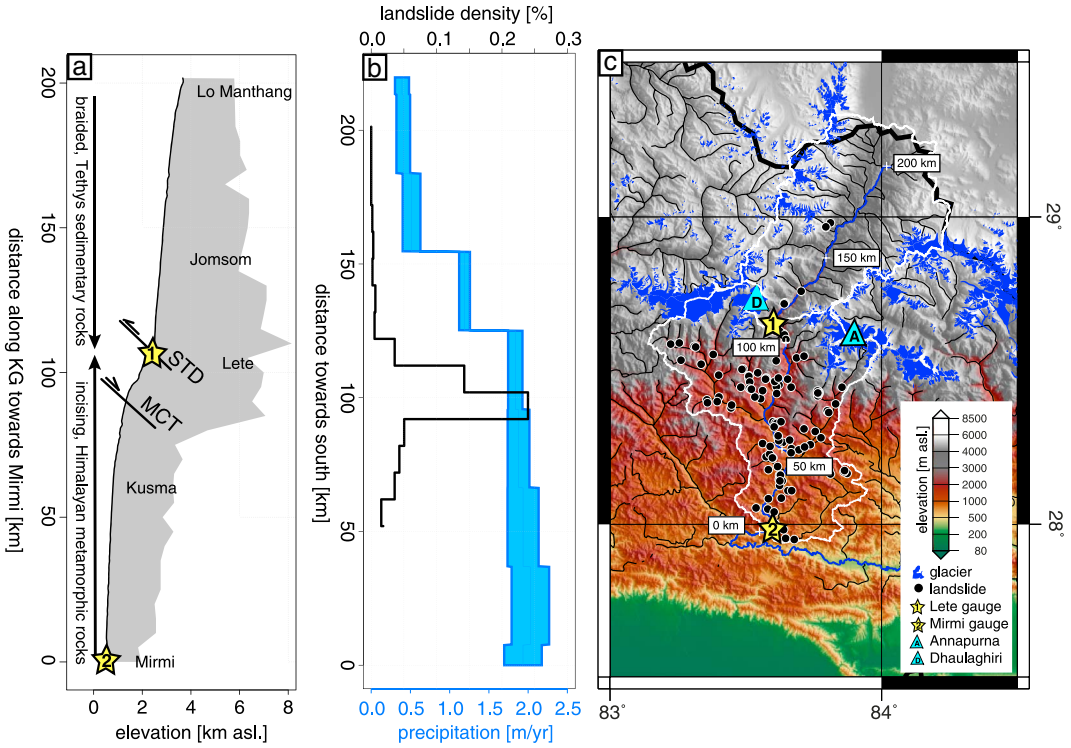

Figure 1. The Kali Gandaki watershed. (a) River longitudinal profile of the KG plotted as distance to Mirmi hydropower facility. South of Lete the basin is characterized by a deeply incising river and to the north by a braided system. Shaded areas represent ridge topography along the river, obtained from 30 km wide swath profiles for 5 km river increments [after *Hergarten et al.*, 2014]. (b) Annual precipitation distribution (blue, mean ± one standard deviation) over the whole map width of Figure 1c, derived from TRMM-3B42 [*Huffman et al.*, 2010] and landslide density distribution (black) plotted against distance toward south. Black landslide density in % area illustrates the occurrence of fresh landslide surfaces mapped between 2006 and 2013. Density is measured over 10 km wide east-west transects (Figure S1). (c) Color-coded DEM strapped over shaded relief map. Dark blue lines are major rivers; KG featured in bold blue line with along-river distance marks in white boxes (distance toward Mirmi). Areas bordered by white lines represent the two basins upstream of the gauging stations.

2. Kali Gandaki Basin

The KG (Figure 1) has a drainage area of ~12000 km^2, straddling the semiarid southern Tibetan Plateau (mean precipitation $P < 500$ mm/yr) and the monsoon-dominated Himalayas ($P \sim 2000$ mm/yr; Figure 1b). These two climatic domains are separated by the High Himalayan orographic barrier including the >8000 m peaks of Dhaulagiri and Annapurna. North of this barrier, the watershed is underlain by Tethyan sedimentary rocks, and the trunk river mostly occupies extensive braid plains flanked by complex terrace staircases cut into the Miocene-Quaternary fill of the Takkhola Graben [*Fort*, 2000; *Adhikari and Wagreich*, 2011]. At least 3.7 km^3 of poorly consolidated sediment are stored in this graben system [*Blöthe and Korup*, 2013], ranging from coarse fan conglomerates to silty backwater deposits, and clay-rich lake beds [*Adhikari and Wagreich*, 2011]. Much of these deposits is pervasively gullied and locally prone to slow, deep-seated landsliding. Downstream, the river has carved narrow, steep gorges through metamorphic rocks of the Higher and Lesser Himalayan sequences [*Lavé and Avouac*, 2001]. Hanging tributary valleys illustrate the ongoing rapid incision of the main stream [*Goode and Burbank*, 2009], and steep bedrock hillslopes directly connect to the fluvial system. Glaciers occupy similar portions (~10%) in both subbasins (Figure 1c), but they were considerably more extensive during the Last Glacial Maximum [*Zech et al.*, 2009].

The Indian Summer Monsoon (ISM) supplies ~80% of the annual precipitation in the central Himalayas over a 4 month period [*Andermann et al.*, 2011], and water and sediment discharge mimic this pattern [*Gabet et al.*, 2008; *Andermann et al.*, 2012a]. Across the Himalayas, intense monsoon rainfall, enhanced by orographic forcing, drives landsliding in threshold topography [*Korup and Weidinger*, 2011], sustained by rapid tectonic shortening [*Lavé and Avouac*, 2001]. Landslides are known to have mobilized up to tens of cubic kilometers of rock

[*Weidinger*, 2006]; however, smaller landslides are much more frequent during the ISM [*Gabet et al*., 2004; *Dahal and Hasegawa*, 2008]. The suspended sediment concentration of Nepalese rivers scales linearly with direct discharge (Q_d) [*Andermann et al*., 2012a], i.e., the fast discharge component generated when intense rainfall exceeds infiltration capacities, rather than with total river discharge (Q). In the central Himalayas roughly two thirds of the river discharge drains through a deep groundwater reservoir [*Andermann et al*., 2012b], but sediment transport in these rivers appears to be dominated by the supply of material through rapid surface drainage during rainstorms [*Andermann et al*., 2012a].

3. Data

We use data from two stations in the KG basin to assess variations in water discharge, sediment concentration (C_s), and caliber on either side of the orographic divide (Table S3 and Text S4-1 in the supporting information). The upper station near Lete village (~2500 m above sea level (asl); Figures 1 and S2) has an upstream area of 3450 km^2. Here twice daily C_s and Q values are available over 2 years (2011–2012). The median grain size, sand (125–2000 μm), and mud (<125 μm, defined as mud for simplification) fractions were obtained from 107 particle size distributions (Text S4). The lower station at Mirmi (520 m asl) is located within the thalweg of the river, ~100 m upstream of the water intake of a run-of-the-river hydropower facility (Nepal Electricity Authority), at an upstream area of 7580 km^2. River discharge is syphoned from November to May, but only a small fraction (~5%) is diverted during the monsoon season. During the low-flow season, the sampling site is located within a backwater-affected river reach, but during ISM river discharge exceeds water diversion by more than an order of magnitude, and the river is free flowing (Figure S5). Daily C_s (separated into sand fraction C_{sand} >125 μm and mud fraction C_{mud} <125 μm), and hourly Q data were collected between 2006 and 2012 (Text S4-1). We used the data for 2011 and 2012 for a direct comparison with Lete station. We separated Q into base flow Q_b, sourced by groundwater and meltwater, and fast-changing direct discharge Q_d, using the recursive digital filter method (BFI_{max}) by *Eckhardt* [2005]. This hydrograph separation technique was successfully applied by *Andermann et al*. [2012a] and *Tolorza et al*. [2014] to assess sediment fluxes. For the KG, it yields important base flow contributions, similar to what has been reported by *Andermann et al*. [2012b] and *Müller et al*. [2014] for Himalayan rivers. We used daily precipitation (P) data from the Tropical Rainfall Measuring Mission (TRMM-3B42, V7) [*Huffman et al*., 2010] for comparison with the discharge components. To assess the spatial pattern of mass wasting, we mapped fresh landslide scars from Landsat 5, 7, and 8 imagery (http://earthexplorer.usgs.gov/, Table S7 and Text S4-2). We mapped surface changes related to fresh scars of deep-seated, catastrophic landslides that occurred between pre- and post-ISM images of each year. We also recorded landslides between post- and pre-ISM images, in order to cover monsoonal and nonmonsoonal periods (Text S4-2).

4. Results

Throughout the KG basin, the bulk precipitation was associated with the ISM (Figures 2 and S6), which contributed ~70% of annual water fluxes at Lete and ~80% at Mirmi (see Table S3). Sediment concentrations mirrored this seasonality, with high C_s of >6 g/L during the ISM and consistently low (C_s < 0.5 g/L) during most other times (Figures 2 and 3). The seasonal granulometry differed clearly between the stations.

At Lete, ~2% of the total suspended sediment transport occurred outside the ISM season. The sand-to-mud ratio (C^*) was 1:2. The monthly median C^* varied little, between 0.3 and 0.5 throughout the year, with a dominant fraction of fines (>50%). On average, 63% of the suspended load had a grain size <63 μm. Measured grain size distributions displayed no seasonal pattern, scattering ~40% (Figure S8). The total estimated suspended sediment flux was 9.7 ± 1.2 megaton (Mt)/yr from 2011 to 2012, of which 6.5 ± 0.8 Mt/yr was mud and 3.2 ± 0.4 Mt/yr was sand.

At Mirmi, <1% of the annual flux occurred outside of the ISM season. Sediment discharge shows seasonal hysteresis, with values of sand, mud, and total suspended sediment concentrations remaining high when Q or P dropped off in the post-ISM period (Figure S8). These effects disappear when comparing corresponding variables to Q_d (Figure S8). At Mirmi, monthly median C^* varied considerably during the ISM seasons, with a nearly fivefold increase from $C^* = 0.2$ in June to $C^* \geq 1.0$ in mid-ISM (Figure 2). During the dry season (Figure 2, grey shading), the sampling location was within the backwater from the hydropower intake. Elevated C^* values during ISM occurred when backwater effects were minimal (unshaded interval in Figure 2). The evolution of C^* over the ISM is not matched by Q, and C^* decreased by September already while Q remained high

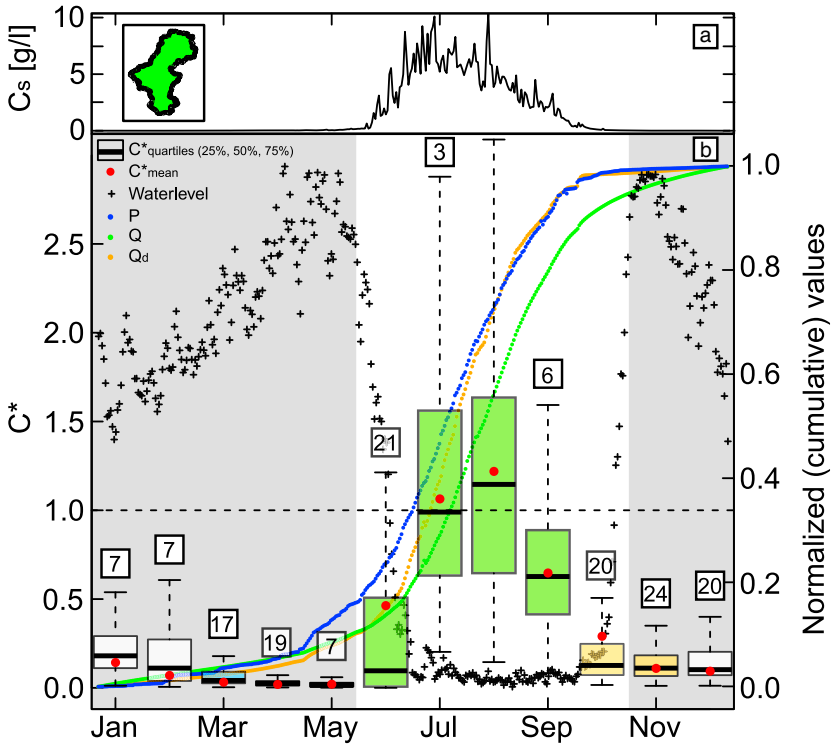

Figure 2. Mirmi daily C_s measurements and hydrology data from 2006 to 2012 (analog to Lete (Figure 3)). (a) Mean daily C_s. Inset indicates upstream basin area. (b) Box plots of monthly mean suspended sand-to-mud concentration ratios C^* (sand >0.125 μm). Red dots and horizontal thick lines are means and medians of C^*, respectively. Boxes enclose first and third quartiles; whiskers span the 1.5-fold interquartile range. Square boxes contain the number of outliers. Color of quartile boxes coded to seasons: white = winter, blue = pre-ISM, green = ISM, and yellow = post-ISM. Dashed line represents equal sand and mud concentrations. Cumulative mean daily precipitation P (blue), discharge Q (dark green), and direct discharge Q_d (orange). Crosses show mean daily water level at intake dam normalized by its average annual sum. Shaded area covers base flow period with regulated streamflow.

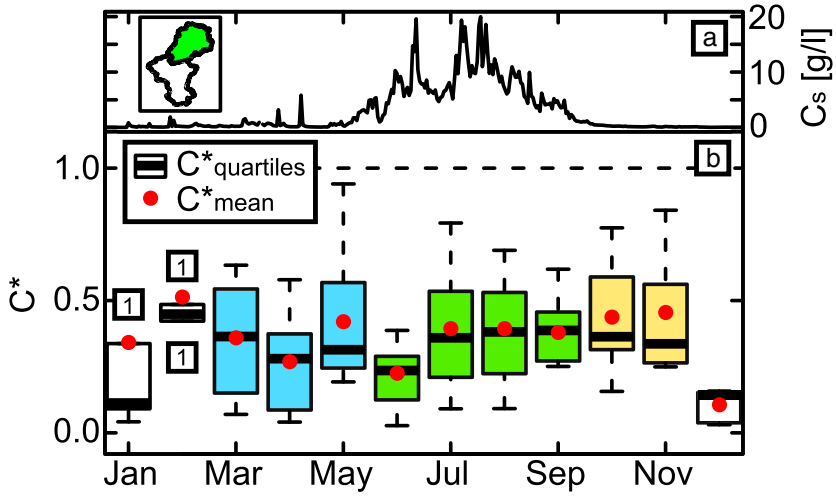

Figure 3. Lete daily C_s measurements June 2011 to November 2012 (analog to Mirmi (Figure 2)). (a) Seasonal pattern of mean daily C_s. Inset shows upstream basin area (shaded in green). (b) Box plots of monthly mean suspended sand-to-mud concentration ratios C^* (sand >0.125 μm). Red dots are mean C^* values and bold black bars median ratios. Dashed line is equal sand and mud concentration. Boxes enclose first and third quartiles; whiskers span the 1.5-fold interquartile range. Square boxes contain the number of outliers.

(Figure 2). At other times, the granulometry of the river load may have been affected by the presence of the dam. The samples contained little material $<63\ \mu m$, with an average of 4.6%. At Mirmi, the average estimated suspended sediment flux from 2011 to 2012 was 30.2 ± 3.2 Mt/yr, of which 18.8 ± 1.2 Mt/yr was mud and 11.4 ± 2.0 Mt/yr was sand. For 2006 to 2012, the average flux was 36.9 ± 10.6 Mt/yr, of which 18.6 ± 3.7 Mt/yr was mud and 18.3 ± 6.9 Mt/yr was sand.

Between 2006 and 2013, seven landslides occurred upstream of Lete and 120 downstream (Figure 1c), all of them during the ISM. During 2011–2012, five landslides occurred upstream of Lete and 40 downstream. Detected landslides affected <0.05% of the surface area upstream of Lete and up to 0.24% downstream (Figure 1b).

5. Discussion

At Lete and Mirmi stations, virtually all suspended sediment transport occurred during the ISM and its immediate aftermath (Figures 2, 3, S6, and S9), with similar trends for both sand and mud. However, the sources and mobilization mechanisms of sediment varied greatly across the basin, embossing a characteristic sediment granulometry.

Upstream of Lete, muddy sediment was prevalent, with a granulometry that was variable during winter when temperatures are lowest. This indicates that glacial production of sediments is not an immediate source of the river load in this part of the basin. Instead, the muds could have been remobilized from the Takkhola Graben fill. Bulk ^{14}C ages of organic matter in fluvial sediment collected upstream of Lete [*Galy and Eglinton*, 2011] attest to potentially long-lived nonglacial sources of sediment in the upper KG. On monthly and longer time scales, the granulometric variability is smoothed toward a steady output of sediment containing ~60% of the $<63\ \mu m$ fraction and ~70% mud. There is no indication that deep-seated, catastrophic landslides are an important source of this sediment, neither in the size distribution of the suspended load nor in the satellite imagery (Figure 1). During field observations in 2014, no landslides were discovered, lending further support to this interpretation.

In contrast, the sand fraction of the river load systematically increases during the ISM at Mirmi (Figure 2). Backwater effects make a complete description of the seasonal cycle difficult; however, the fivefold increase of C^* within ISM is significant. The seasonal contrast is also supported by bulk suspended sediment data [*Andermann et al.*, 2012a] predating the dam construction. These data demonstrate that backwater has only little impact on the seasonality of the suspended load. Suspended sediment transport at Mirmi is driven by direct discharge Q_d, not total discharge Q (Figure S8), implying that the sediment load of the KG and its granulometry are not set by river flow conditions. Instead, the observed coarsening and increasing concentrations of all suspended sediment fractions are correlated with changes of direct discharge, which depends on precipitation intensity [*Andermann et al.*, 2012a]. This indicates that suspended sediment load and caliber at Mirmi during the ISM are linked to precipitation-driven processes in the southern Himalayas, downstream of Lete. Furthermore, most of the sediment carried by rivers in the Nepal Himalayas does not seem to result from anthropogenic soil degradation. *Gallo and Lavé* [2014] demonstrated that landslides in a Himalayan headwater catchment dominate the erosional work, while soil-mantled hillslopes do not release any relevant volumes of sediments. Similarly, we attribute the observed shifts in sediment granulometry during the ISM to mass wasting of fresh hillslope materials with larger clasts. Mass wasting processes are widely documented across the High Himalayas and are major sources of sediment [*Gabet et al.*, 2008; *Gallo and Lavé*, 2014]. Fresh landslide scars almost exclusively form during the ISM season along the wet, south facing Himalayan front (Figure 1c), a pattern also evident in the recorded timing of >700 well-documented landslides all over Nepal [*Dahal and Hasegawa*, 2008; *Kirschbaum et al.*, 2009] (Figure 4).

The mean erosion rate inferred from the sediment fluxes recorded between 2011 and 2012 upstream of Lete is surprisingly high (1.0 ± 0.1 mm/yr) and highlights the importance of the Thakkhola Graben fill as a potentially major sediment source. For the whole basin the suspended sediment-derived erosion rate was 1.9 ± 0.2 mm/yr and 2.5 ± 0.9 mm/yr for the monsoon-prone Himalayan section between Lete and Mirmi. These values are consistent with independent estimates from this area [*Andermann et al.*, 2012a; *Lupker et al.*, 2012]. The increased erosion rate in the downstream part of the catchment may well reflect the sediment supply from intense mass wasting.

Volumetrically, the entire $<63\ \mu m$ load of the KG River at Mirmi can be explained by export from the Tibetan part of the basin as recorded at Lete. Moreover, ~35% of the mud fraction ($<125\ \mu m$) gauged at Mirmi may

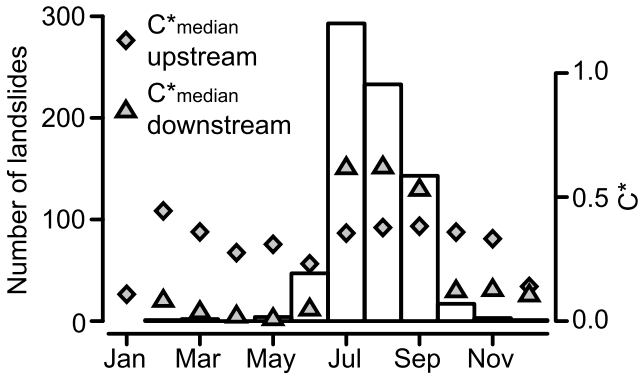

Figure 4. Landslide occurrence histogram. Temporal occurrence distribution of 744 documented landslides in Nepal (1951 to 2007) [from *Dahal and Hasegawa*, 2008; *Kirschbaum et al*., 2009]. Median suspended sand-to-mud concentration ratios C^* at Lete (diamonds) and Mirmi (triangles) are plotted for the period 2011–2012.

stem from the upper, dry part of the basin. Much of this material might derive from the Thakkhola Graben fill, thus projecting the characteristics of this Miocene-Pleistocene sedimentary system onto the present-day Himalayan erosion flux. In contrast, about 70–80% of the sand traveling in suspension at Mirmi is likely to be sourced directly from bedrock or relatively young colluvial deposits in hillslopes of the southern Himalayan front. If the different grain sizes resegregate due to downstream sorting, then grain size populations that were convolved by accumulation along the KG River may be well sorted along the alluvial continuation of the river in the Indian foreland. This can affect the record of mountain processes in distant depocenters, with coarser, sandy deposits in the Gangetic foreland primarily registering the exhumation of the southern Himalayan flank by mass wasting and trans-Himalayan muds affecting accumulation of deposits farther down the Gangetic plains and distal deposition in the Bay of Bengal. Sediment archives are often interpreted according to volumetric thickness of particular layers and attributed to the most obvious source area [e.g., *Métivier et al*., 1999]. Our results demonstrate that it is important to combine particle size with provenance analysis to better pinpoint the source areas [*Goodbred et al*., 2014], especially for inferring large-scale climate variations from intense erosion phases [*Clift et al*., 2008].

6. Conclusions

Grain size information contained in C_s fluxes hold valuable though often overlooked information to probe into the mechanisms of source-to-sink sediment cycles from fast-eroding orogens. Daily records of C_s support previous findings of downstream coarsening across the Himalayan range from bed load size distributions [*Attal and Lavé*, 2006] and add a new temporal component to these observations, demonstrating that the classical downstream fining of sediments is not applicable for monsoonal trans-Himalayan rivers. Instead, downstream coarsening of C_s in the KG River is linked to sediment input by hillslope mass wasting processes, which are almost exclusively associated with the ISM season and the dissected southern Himalayan front. We demonstrate that supply of sediments in the Himalayas to first order depends on hillslope-channel connectivity and the availability of water and how it is portioned over space and time into river discharge. Our findings stress the importance to better understand sediment supply and hillslope-channel connectivity in mountain headwaters for the interpretation of C_s records and depositional archives.

Acknowledgments
This study was funded in part by the Potsdam Research Cluster for Georisk Analysis, Environmental Change and Sustainability (PROGRESS), by the student mobility grant (PROMOS) from the German Academic Exchange Service, and the Helmholtz Postdoc Program (PD-039) from the German Helmholtz Association. The authors like to thank the Lete-Koban hydropower feasibility project, managed through Ambeshwar Engineering Hydropower Pvt. Ltd. and the Kali Gandaki "A" Hydroelectric Project for sharing the data. We used the *R* software environment (http://www.r-project.org/), GIS using open source GRASS GIS (http://grass.osgeo.org), and the generic mapping tool GMT (http://www.gmt.soest.hawaii.edu/). Three constructive reviews have greatly helped to improve the manuscript.

The Editor thanks two anonymous reviewers for their assistance in evaluating this paper.

References

Adhikari, B. R., and M. Wagreich (2011), Provenance evolution of collapse graben fill in the Himalaya—The Miocene to Quaternary Thakkhola-Mustang Graben (Nepal), *Sediment. Geol.*, *233*(1–4), 1–14, doi:10.1016/j.sedgeo.2010.09.021.

Andermann, C., S. Bonnet, and R. Gloaguen (2011), Evaluation of precipitation data sets along the Himalayan front, *Geochem. Geophys. Geosyst.*, *12*, doi:10.1029/2011GC003513.

Andermann, C., A. Crave, R. Gloaguen, P. Davy, and S. Bonnet (2012a), Connecting source and transport: Suspended sediments in the Nepal Himalayas, *Earth Planet. Sci. Lett.*, *351–352*, 158–170.

Andermann, C., L. Longuevergne, S. Bonnet, A. Crave, P. Davy, and R. Gloaguen (2012b), Impact of transient groundwater storage on the discharge of Himalayan rivers, *Nat. Geosci.*, *5*(2), 127–132, doi:10.1038/ngeo1356.

Attal, M., and J. Lavé (2006), Changes of bedload characteristics along the Marsyandi River (central Nepal): Implications for understanding hillslope sediment supply, sediment load evolution along fluvial networks, and denudation in active orogenic belts, *Tecton. Clim. Landscape. Evol.*, *2398*(09), 143, doi:10.1130/2006.2398(09).

Blöthe, J. H., and O. Korup (2013), Millennial lag times in the Himalayan sediment routing system, *Earth Planet. Sci. Lett.*, *382*, 38–46, doi:10.1016/j.epsl.2013.08.044.

Brummer, C. J., and D. R. Montgomery (2003), Downstream coarsening in headwater channels, *Water Resour. Res.*, *39*(10), 1294, doi:10.1029/2003WR001981.

Clift, P. D., K. V. Hodges, D. Heslop, R. Hannigan, H. Van Long, and G. Calves (2008), Correlation of Himalayan exhumation rates and Asian monsoon intensity, *Nat. Geosci.*, *1*(12), 875–880, doi:10.1038/ngeo351.

Dahal, R., and S. Hasegawa (2008), Representative rainfall thresholds for landslides in the Nepal Himalaya, *Geomorphology*, *100*(3–4), 429–443, doi:10.1016/j.geomorph.2008.01.014.

Eckhardt, K. (2005), How to construct recursive digital filters for baseflow separation, *Hydrol. Process.*, *19*(2), 507–515, doi:10.1002/hyp.5675.

Fort, M. (2000), Glaciers and mass wasting processes: Their influence on the shaping of the Kali Gandaki valley (higher Himalaya of Nepal), *Quat. Int.*, *65-66*(1), 101–119, doi:10.1016/S1040-6182(99)00039-7.

Gabet, E., D. W. Burbank, J. K. Putkonen, B. A. Pratt-Sitaula, and T. Ojha (2004), Rainfall thresholds for landsliding in the Himalayas of Nepal, *Geomorphology*, *63*(3–4), 131–143, doi:10.1016/j.geomorph.2004.03.011.

Gabet, E., D. Burbank, B. A. Pratt-Sitaula, J. Putkonen, and B. Bookhagen (2008), Modern erosion rates in the High Himalayas of Nepal, *Earth Planet. Sci. Lett.*, *267*(3–4), 482–494, doi:10.1016/j.epsl.2007.11.059.

Gallo, F., and J. Lavé (2014), Evolution of a large landslide in the High Himalaya of central Nepal during the last half-century, *Geomorphology*, doi:10.1016/j.geomorph.2014.06.021.

Galy, V., and T. Eglinton (2011), Protracted storage of biospheric carbon in the Ganges–Brahmaputra basin, *Nat. Geosci.*, *4*(12), 843–847, doi:10.1038/ngeo1293.

Goodbred, S. L., P. M. Paolo, M. S. Ullah, R. D. Pate, S. R. Khan, S. A. Kuehl, S. K. Singh, and W. Rahaman (2014), Piecing together the Ganges-Brahmaputra-Meghna River delta: Use of sediment provenance to reconstruct the history and interaction of multiple fluvial systems during Holocene delta evolution, *Geol. Soc. Am. Bull.*, doi:10.1130/B30965.1.

Goode, J. K., and D. W. Burbank (2009), Numerical study of degradation of fluvial hanging valleys due to climate change, *J. Geophys. Res.*, *114*, F01017, doi:10.1029/2007JF000965.

Hergarten, S., J. Robl, and K. Stüwe (2014), Extracting topographic swath profiles across curved geomorphic features, *Earth Surf. Dyn.*, *2*(1), 97–104, doi:10.5194/esurf-2-97-2014.

Huffman, G. J., R. F. Adler, D. T. Bolvin, and E. J. Nelkin (2010), The TRMM Multi-Satellite Precipitation Analysis (TMPA), in *Satellite Rainfall Applications for Surface Hydrology*, edited by F. Hossain and M. Gebremichael, Springer, Netherlands.

Kirschbaum, D. B., R. Adler, Y. Hong, S. Hill, and A. Lerner-Lam (2009), A global landslide catalog for hazard applications: Method, results, and limitations, *Nat. Hazards*, *52*(3), 561–575, doi:10.1007/s11069-009-9401-4.

Korup, O., and J. T. Weidinger (2011), Rock type, precipitation, and the steepness of Himalayan threshold hillslopes, *Geol. Soc. London, Spec. Publ.*, *353*(1), 235–249, doi:10.1144/SP353.12.

Lavé, J., and J. Avouac (2001), Fluvial incision and tectonic uplift across the Himalayas of central Nepal, *J. Geophys. Res.*, *106*(B11), 26,561–26,591, doi:10.1029/2001JB000359.

Lupker, M., P.-H. Blard, J. Lavé, C. France-Lanord, L. Leanni, N. Puchol, J. Charreau, and D. Bourlès (2012), 10Be-derived Himalayan denudation rates and sediment budgets in the Ganga basin, *Earth Planet. Sci. Lett.*, *333–334*, 146–156, doi:10.1016/j.epsl.2012.04.020.

Marshall, J. A., and L. S. Sklar (2012), Mining soil databases for landscape-scale patterns in the abundance and size distribution of hillslope rock fragments, *Earth Surf. Processes Landforms*, *37*(3), 287–300, doi:10.1002/esp.2241.

Métivier, F., Y. Gaudemer, P. Tapponnier, and M. Klein (1999), Mass accumulation rates in Asia during the Cenozoic, *Geophys. J. Int.*, *137*(2), 280–318, doi:10.1046/j.1365-246X.1999.00802.x.

Müller, M. F., D. N. Dralle, and S. E. Thompson (2014), Analytical model for flow duration curves in seasonally dry climates, *Water Resour. Res.*, *50*(7), 5510–5531, doi:10.1002/2014WR015301.

Paola, C., and R. Seal (1995), Grain size patchiness as a cause of selective deposition and downstream fining, *Water Resour. Res.*, *31*(5), 1395–1407, doi:10.1029/94WR02975.

Tolorza, V., S. Carretier, C. Andermann, F. Ortega-culaciati, L. Pinto, and M. Mardones (2014), Contrasting mountain and piedmont dynamics of sediment discharge associated with groundwater storage variation in the Biobío River, *J. Geophys. Res. Earth Surf.*, *119*, 2730–2753, doi:10.1002/2014JF003105.

Turowski, J. M., D. Rickenmann, and S. J. Dadson (2010), The partitioning of the total sediment load of a river into suspended load and bedload: A review of empirical data, *Sedimentology*, *57*(4), 1126–1146, doi:10.1111/j.1365-3091.2009.01140.x.

Weidinger, J. T. (2006), Predesign, failure and displacement mechanisms of large rockslides in the Annapurna Himalayas, Nepal, *Eng. Geol.*, *83*(1–3), 201–216, doi:10.1016/j.enggeo.2005.06.032.

Wulf, H., B. Bookhagen, and D. Scherler (2012), Climatic and geologic controls on suspended sediment flux in the Sutlej River Valley, western Himalaya, *Hydrol. Earth Syst. Sci.*, *16*(7), 2193–2217, doi:10.5194/hess-16-2193-2012.

Zech, R., M. Zech, P. W. Kubik, K. Kharki, and W. Zech (2009), Deglaciation and landscape history around Annapurna, Nepal, based on 10Be surface exposure dating, *Quat. Sci. Rev.*, *28*(11–12), 1106–1118, doi:10.1016/j.quascirev.2008.11.013.